ILASS 2008
Sep. 8-10, 2008, Como Lake, Italy

Paper ID ILASS08-14-2

PRELIMINARY RESULTS ON THE EFFECT OF PHASE ANGLE ON COAXIAL JET BEHAVIOR SPANNING SUB- TO SUPERCRITICAL PRESSURES

Ivett A Leyva*, Juan I Rodriguez°, Bruce Chehroudi+, Douglas Talley*

*AFRL/RZSA Edwards AFB, Ca,
°Graduate Student, UCLA, Los Angeles, Ca
+ ERC, Edwards AFB, Ca

ABSTRACT

This paper describes the effects of phase angle of an acoustic pressure field on a shear coaxial jet. The jet is forced with a transverse acoustic field, made up of two acoustics sources with p'_{RMS}/pmean up to 4%. The chamber pressure ranges from 1.5 to 5.0 MPa. The momentum flux ratio (MR) between the outer and inner jet varies from 0.02 to 23 and the velocity ratio from 0.25 to 23. The shear coaxial geometry is selected because of its application to liquid rocket engines. The jet was analyzed by taking high speed images and exit-plane temperature measurements. This work continues previous work where the jet was excited with one acoustic source; therefore the jet location was fixed with respect to the acoustic field. For all pressure regimes, the cases with MR > 9 were least sensitive to the acoustic field. That is, the percentage variation of the dark core length with respect to the baseline was least. At nearcritical pressures, for MR ~ 1 to 5, it appears that the dark core length is more affected, in terms of its reduction, by high acoustic velocity amplitude and not high acoustic pressure amplitudes.

INTRODUCTION

The motivation for this work springs from the problem of combustion instabilities in liquid rocket engines. One of the unit physics problems that can be defined to try to understand the larger problem of combustion instabilities is the interaction of an acoustic field with a typical rocket injector. We first investigate a coaxial injector because they are widely used in liquid rocket engines (LRE's). A key advantage of coaxial jets is that as the Momentum Flux Ratio (MR) between the outer jet and the inner jet increases, mixing between the two jets increases so that uniformity can be obtained in relatively short distances from the exit plane. We focus on a transverse acoustic field because the interaction of this type of field with an injector is one of the most destructive ones to a rocket engine. Recently, Richecoeur et al. [1] studied the problem of transverse acoustics with three $CH_4/0_2$ coaxial injectors at a chamber pressure of 0.9 MPa. They observed that the combustion process is more sensitive to acoustics at low outer jet velocities (CH_4).

The Space Shuttle Main Engine (SSME) and the Vulcan engine for the Ariane 5 are examples of LRE's designed to operate above the critical pressures of each propellant individually. Hence, in our studies, we vary the chamber pressure from sub to supercritical values. In a typical application of a coaxial injector for a LOX/LH2 engine (e.g. SSME), the oxygen is injected at subcritical temperatures in the center jet while the hydrogen is injected at supercritical temperatures, after being used as a coolant for the engine nozzle, in the coaxial jet. For these flows, the mixture no longer has a singular critical point but rather there are critical mixing lines that define its thermodynamic state [2]. Because of the added complexity introduced when working with mixtures, N_2 is used as the sole working fluid in this study. A typical operating velocity ratio (VR) between the outer and inner jets in a coaxial injector is around 10 or higher, arrived at from empirical evidence that injectors operating at these high VR's are more stable against combustion instabilities [3]. Therefore in our studies we vary VR and MR from less than 1 to the low 20's for both variables.

This paper is focused specifically on the effects of the phase of the acoustic pressure and velocity field on the coaxial jet flow. In previous experiments performed in the same lab there was one acoustic source at one end of the test chamber and a non-movable reflective wall at the other end. This meant that the relation of the position of the jet with respect to the acoustic wave profile was fixed. By adding a second identical acoustic source the magnitude and relative position of the pressure and velocity acoustic field with respect to the jet are now varied. Preliminary results for a few run conditions were presented before in the papers by Leyva et. al. [4] and Rodriguez et. al. [5]. This paper presents a complete set of data for one geometry. The data includes three chamber pressures and several MR's for each pressure. The axial length of the dark core is the main metric studied in this paper. An analysis of the spreading angle of the inner and outer jet under an acoustic field will be the next metric to be analyzed in a future paper.

EXPERIMENTAL SETUP

The experiments detailed here were performed at the Cryogenic Supercritical Laboratory (EC-4) at the Air Force Research Laboratory (AFRL) at Edwards Air Force Base, Ca. Figure 1 shows the main chamber and the supporting systems. In the current setup, ambient temperature N_2 is used to supply the inner and outer jet and also to pressurize the chamber. As a note, the critical temperature of N_2 is 126.2 K

and its critical pressure is 3.39 MPa. Both the inner and the outer jets are cooled by heat exchangers (HE's) using liquid nitrogen obtained from a cryogenic tank. One heat exchanger cools the inner jet and other two cool the outer jet. Depending on the setup, one of these HE's can be bypassed to modify the cooling patterns. The mass flow rates of liquid nitrogen through the HE's are regulated in order to control the temperature of the jets. These rates are measured with Porter® mass flow meters (122 and 123-DKASVDAA) at ambient conditions to avoid difficulties with mass flow rate measurement at cryogenic temperatures. An inner chamber was built and housed inside the main chamber to maintain the amplitude of the acoustic oscillations to a maximum at the test section. The inner chamber is 6.6 cm high, 7.6 cm wide and 1.3 cm deep (see Fig. 1).

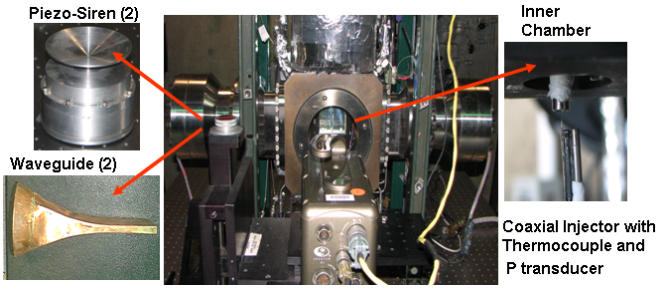

Figure 1. Experimental setup

The inner tube making the inner jet has an inner diameter, D1, of 0.51 mm with length-to-diameter ratio of 100. The inner jet exit plane is recessed by 0.25 mm from the outer jet. The outer annular jet's inner diameter, D2, is 1.59 mm with outer diameter, D3, of 2.42 mm. For the outer jet, the length-to-mean-width of the annular passage is 67. The coaxial injector is shown in Fig. 2.

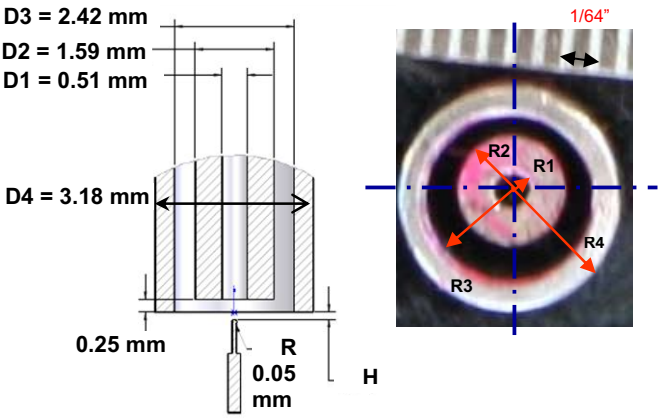

Figure 2. Details on the geometry of the shear coaxial injector used in this study.

The chamber pressure is measured with a Stellar 1500 transducer. An unshielded type E thermocouple with a bead diameter of 0.1 mm is used to measure the temperature of the jets. The accuracy of this thermocouple was checked with an RTD and found to be ± 1 K. Also, a Kulite® XQC-062 pressure transducer is used to measure the pressure near the location of the thermocouple tip at a sampling frequency of 20 kHz (see right picture in Fig. 1). Both the pressure transducer and the thermocouple are moved in the plane perpendicular to the jet axis with two linear positioning stages built by Atto**cube** Systems AG. Each stage has a range of about 3 mm in 1 dimension with step sizes in the order of 0.01 mm. One stage was placed on top of the other with their axis of movement perpendicular to each other for a total maximum interrogation area of 3 mm by 3 mm. The thermocouple and pressure transducer were fixed to a custom made probe stand mounted on top of the positioning assembly. In turn, the linear stages were placed at the top end of a shaft that rested on a large 10-cm range linear stage built by SETCO™ outside the main chamber. Thus, the temperature probe approaches the coaxial jet from the bottom and it can get arbitrarily close to the exit plane. This thermocouple has even been used to measure the temperature within the recess of the inner jet.

The density, viscosity, and surface tension from the measured flow rates, chamber pressure and jet temperature are obtained using NIST's REFPROP© database [6-7]. From these properties, Re, We, outer to inner jet velocity ratio (VR) and MR for a given condition are then calculated. The coaxial flow was visualized using a Phantom® 7.1 CMOS camera. The camera can be seen facing the main chamber in the center picture of Fig. 1. Backlit images with a resolution from 128x224 to 196x400 pixels were obtained, with each pixel representing an area of approximately 0.08 mm by 0.08 mm. The framing rate was 20-25 kHz. The number of images saved per run was 1000 on average. The jet was backlit using a Newport® variable power arc lamp set at 160 W.

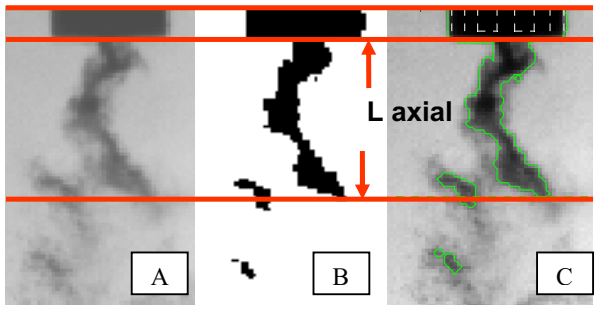

Figure 3. Definition of axial dark core length, L axial. [A] typical image. [B] original image after it has been thresholded to a binary image. [C] contour from which the axial length is calculated

The dark core lengths are measured from 998 images using a MATLAB® subroutine based on the Otsu technique [8] to find a grayscale threshold which helps distinguish the inner core from the rest of the image (see Fig. 3). More details on how the dark core is defined and measured are given in previous papers from this group [9-10]. Basically, in our study the inner jet is colder than the outer jet and it appears as a dark central feature on the images. The axial dark core length, L axial, is the projection of the inner jet before its first break along the axis parallel to the jet flow. Although we use the dark core length as the main metric in this study, a note needs to be made that there is not a unique definition for this parameter. The absolute magnitude depends on how the dark core is measured and defined. In this study, we place more value on the trends and relative changes on the dark core as we change operating conditions. We are interested in the dark core length as a qualitative indicator of mixing between the two jets.

The two piezo-sirens used to generate the transverse acoustic field were custom-designed by Hersh Acoustical Engineering, Inc. (see Fig. 1). The principle by which the piezo-sirens work as acoustic drivers is relatively simple. A sinousoidal voltage signal moves a piezo element with an aluminum cone attached to it, which in turn produces acoustics waves. When the two drivers have a zero degree phase angle difference they move in opposite directions. On the contrary, when the two drivers have a 180-degree phase difference the cones move in the same direction, or they 'chase' each other. This behavior is represented by the sketches in Fig. 4. A Fluke® signal generator was used to drive the piezo-sirens with a sinusoidal wave at a chosen driving frequency and phase angle between them. The frequency was manually varied until the highest amplitudes of the pressure waves were obtained. These frequencies spanned a range between 2.93 and 3.09 kHz. Then the signals were amplified and fed to the piezo-sirens. The voltage supplied to each driver was kept constant. A waveguide with a catenary contour was used to guide the waves from a circular cross-section at the end of the aluminum cone to the rectangular cross-section of the rectangular inner chamber.

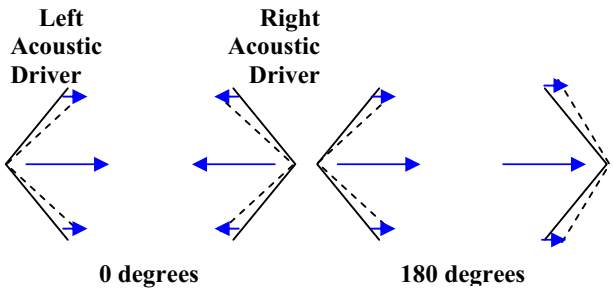

Figure 4. Simplified diagram of the two acoustic drivers at a 0° and 180° phase angle.

RESULTS

A series of runs were made at three nominal chamber pressures (1.5, 3.6, and 5.0 MPa) to span sub to supercritical chamber pressures. The detailed list of run conditions is shown in Table 1 in the appendix. For each chamber pressure several MR's were taken and for each MR the two acoustic sources were run at phase angles from 0 to 360 degrees at intervals of 45 degrees. A qualitative sample of how the jet behaves for the different phase angeles is first shown in Fig. 5. Here the first figure shows the jet with no acoustics. In this case (sub3), the pressure is subcritical and the inner jet is a liquid within 1 or 2 degrees K of the saturation temperature, and the outer jet is a gas. We can see that the dark core, or inner jet, is longest for the case with no acoustics, or baseline. When the acoustic field is turned on (0 degrees), the jet is affected by the acoustics and the inner core is bent and shortened. We can also see how the outer jet is bent compared to the baseline case but not as dramatically. The bending and shortnening of the dark core continues as the phase angle is increased. The minimum dark core length and most bending (qualitatively measured by the horizonal extent of the inner jet travel) are achieved at around 135-180 degrees where we expect to have the highest amplitude of the velocity field.

The results on the shortening of the dark core length for all the cases run are compiled in Fig. 6. In this case, the y axis is the axial dark core length non-dimensionalized by the inner diameter of the inner jet, D1. The x-axis represents the phase angle between the two acoustic sources. The error bars shown are $\pm 1\sigma$. In general, $\sigma \leq$ 20% of the mean. As a convention, the angle is only changed on the right source with respect to the left source (Fig.1). The leftmost point in every graph corresponds to the case where no acoustics were on. In previous papers [9-10] it was shown that as the MR increases the axial dark core length decreases regardless of the chamber pressure. However, the behavior of the dark core length falls in two branches, one for subcritical pressure in which L ~ A/MR^0.2 and the other for near and supercritical pressures where L ~ B/MR^0.5. The results obtained here for the case of no-acoustics agree with those previous results.

Overall, we observe that for the chamber pressures studied here, as MR increases the axial length decreases for all phase angles. For MR >~9, L/D1 is < ~7 for the three chamber pressures and phase angles presented here. The absolute (as compared to percentage) variation of the dark core length with respect to the baseline case as a function of phase angle decreases with MR. Also, as MR increases the curves become more and more flat – less effect of phase angle. For the cases of subcritical and nearcritical pressures, we observe a grouping in the data. In the subcritical case, for MR<1 the lengths are longest as mentioned previously. For the three cases from MR=1 to MR=4.2, we see very good agreement among these cases. The L/D values cluster around 9 to 13 and they have about the same shape. Their mininum occurs around 180 degrees and their maximum around 315-360 degrees. This is consistent with previous observations that the jet is more affected by high velocity fields than by high pressure fields. For the cases we ran with MR>9, the data becomes less sensitive to phase angle.

For the case of nearcritical pressures, the values of L/D for MR=0.55 are the longest. The four curves corresponding to MR=1.0 to 2.1 cluster around each other and show the same curvature. In this case also, the minimum is around 180 degrees and the maximum is around the ends of the curve. Note that while the case for MR=2.9 follows the same curvature as these three cases, because the values for L/D are lower, it clusters better with the high MR curves. For the case of supercritical pressure, the curves for MR=2.4 and above cluster together because of their low L/D's. Note that for near and supercritical pressures the dark core length varies by an order of magnitude between the lowest and highest MR run.

Another way to look at the effect of the phase angle on the dark core length is to look at the ratio of the new dark core with acoustics to the baseline value with no acousitcs. The results are shown in Fg. 7. The data and legend is the same as in the previous figure but for each MR, the dark core lengths with acoustics are normalized by their respective baseline value. This is done to see if as the dark core length becomes shorter with MR, its percentage decrease with acoustics also diminishes. As it turns out, we

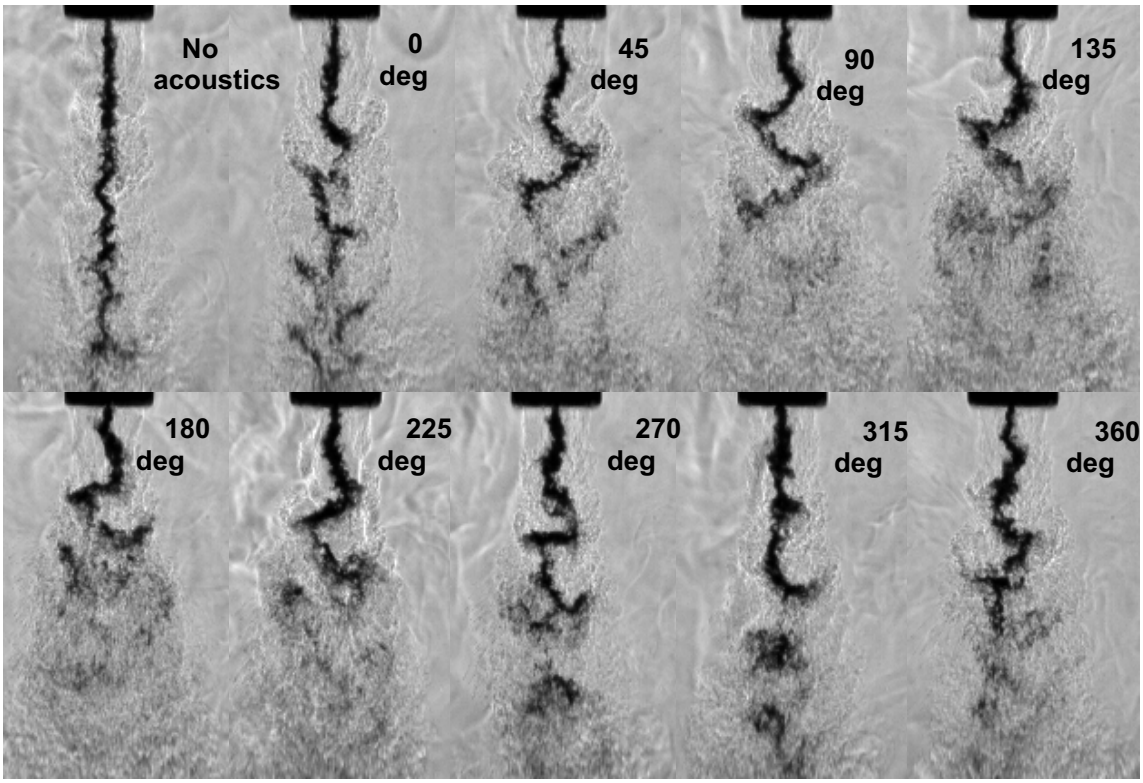

Figure 5. Images of a shear coaxial jet flow for different phase angles between two acoustic sources (case sub3).

see that for all the pressures, when MR is larger than ~9, the change in length for all phase angles varies up to 20%. The biggest percentage reductions are for MR around 1 to 3.

This is consistent with previous data reported in papers [9-10] where the maximum effect of a single acoustic source on the axial dark core length was found to be for ~1<MR<~4. Plotting the data in this way reveals that while the absolute variation of the dark core length for a given MR is usually greater for subcritical pressures, the percentage change for the MR's explored in this study is about the same for the three pressures studied. That is, the percentage change of the axial dark core length seems to be no greater than 50% for all cases. This is even more striking given that p'rms/pchamber is much lower for near and supercritical pressures than for subcritical pressures (Table 1). We also note that the plot of supercritical pressures shows the most scatter on the data.

Since we are varying the phase of the acoustic field with respect to the jet's exit, it is interesting to find out if the dark core length directly responds to the variations of the acoustic field. That is, as the acoustic pressure, p', monotonically increases at the injector location, does the dark core length also monotonically increase or decrease? To answer this question, let's look in detail to a sample of superimposed traces of the normalized magnitude of the acoustic pressure (p' rms/pchamber) and the normalized dark core length (L/D1 axial) as a function of the phase angle. We will look in detail to some nearcritical cases. The results are shown in Figure 8. In general, the change on the location of the minimum in the p' field is due in part to the different frequencies used to drive the acoustic sources. The frequency was chosen to give the maximum amplitudes in both drivers. The maximum p' amplitudes were within 3 kPa for all the nearcritical cases.

For the first case, MR=0.55, VR=2.0 we can see that the decrease on the dark core length when the acoustics are turned on is statistically significant for all phase angles (except perhaps for 225 degrees). However, qualitatively, the trend of L/D does not follow the trend of p', which has a minimum at around 135 degrees. As a note, the inaccuracy of the acoustic pressure is not shown but it is ± 6.9 kPa according to the manufacturer. Therefore, the pressure variations fall within the accuracy of the transducer. The trends on p' although mostly qualitative, agree very well with intuition where we would expect a minimum in acoustic pressure around 180 degrees. In general, it is not surprising not to see a qualitative agreement on the trends of the acoustic pressure and the dark core length since we have seen before that coaxial jets with MR<1 do not seem very sensitive to the acoustic fields produced with the current setup.

The second case to consider has MR=1.6, VR=2.8. The qualitative trends of L/D and p' agree with each other. Within the error bars we have the maximum L/D at the same phase angles where we have a maximum in the p' field (45, 90 degrees). This would mean that when the pressure disturbance is maximum, the jet gets disturbed the least. Similarly the minimum L/D happens close to the minimum p' (shifted by 45 degrees). This also points to the observation that it is the velocity fluctuations that most affect the jet. That is, when u' is highest, hence p' is lowest, the inner jet core decreases and bends the most. Notice also that p' for 0 degrees and 360 degrees are very close to each

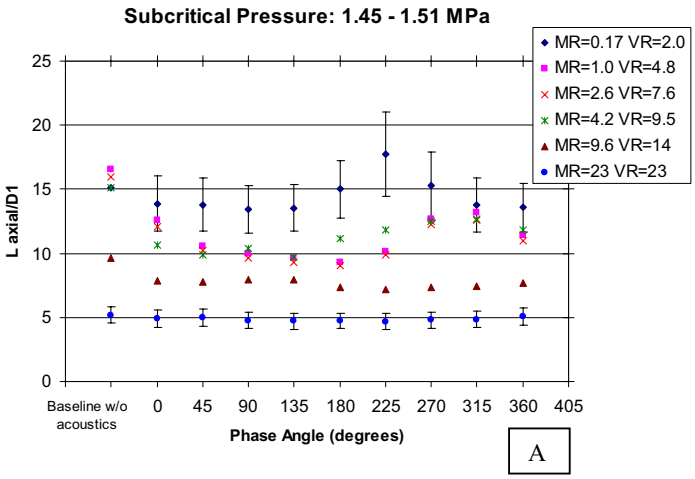

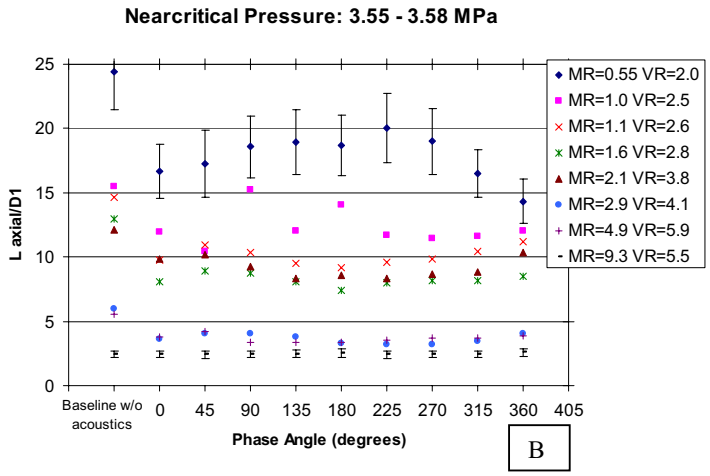

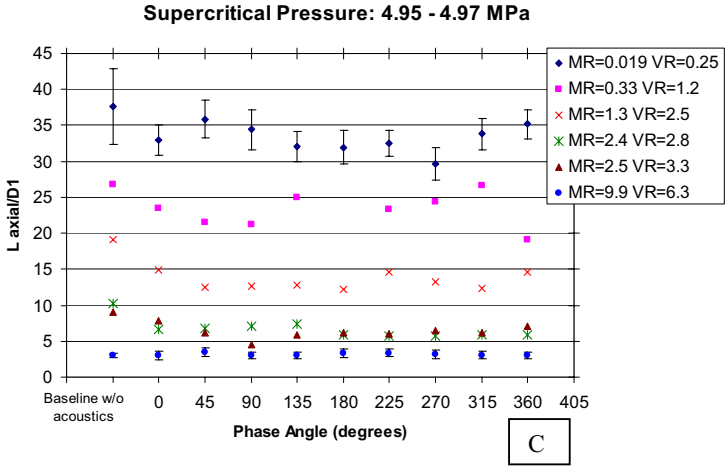

Figure 6. Axial dark core length normalized by the inner jet diameter as a function of the phase angle for [A] Subcritical pressure, [B] Nearcritical pressure and [C] Supercritical pressure

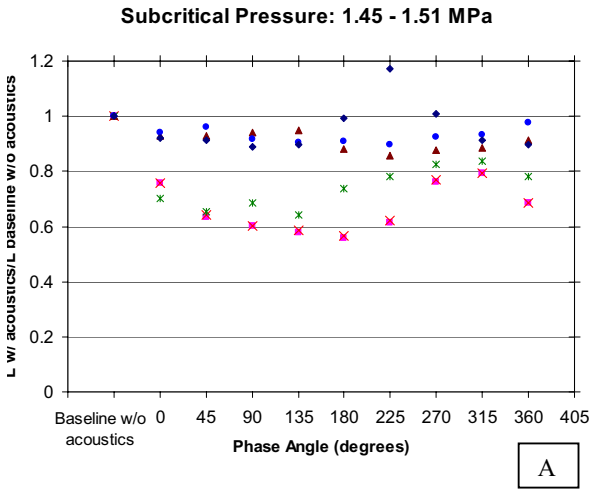

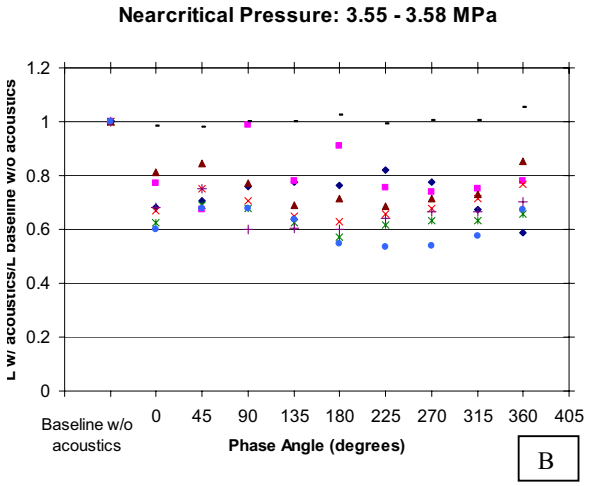

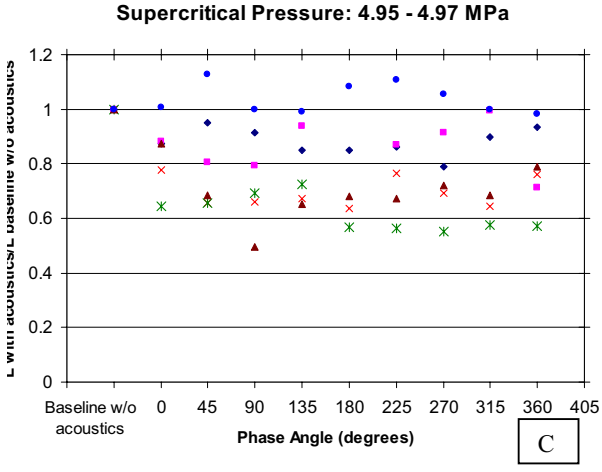

Figure 7. Axial dark core length normalized by baseline value with no acoustics as a function of the phase angle [A] Subcritical pressure, [B] Nearcritical pressure and [C] Supercritical pressure

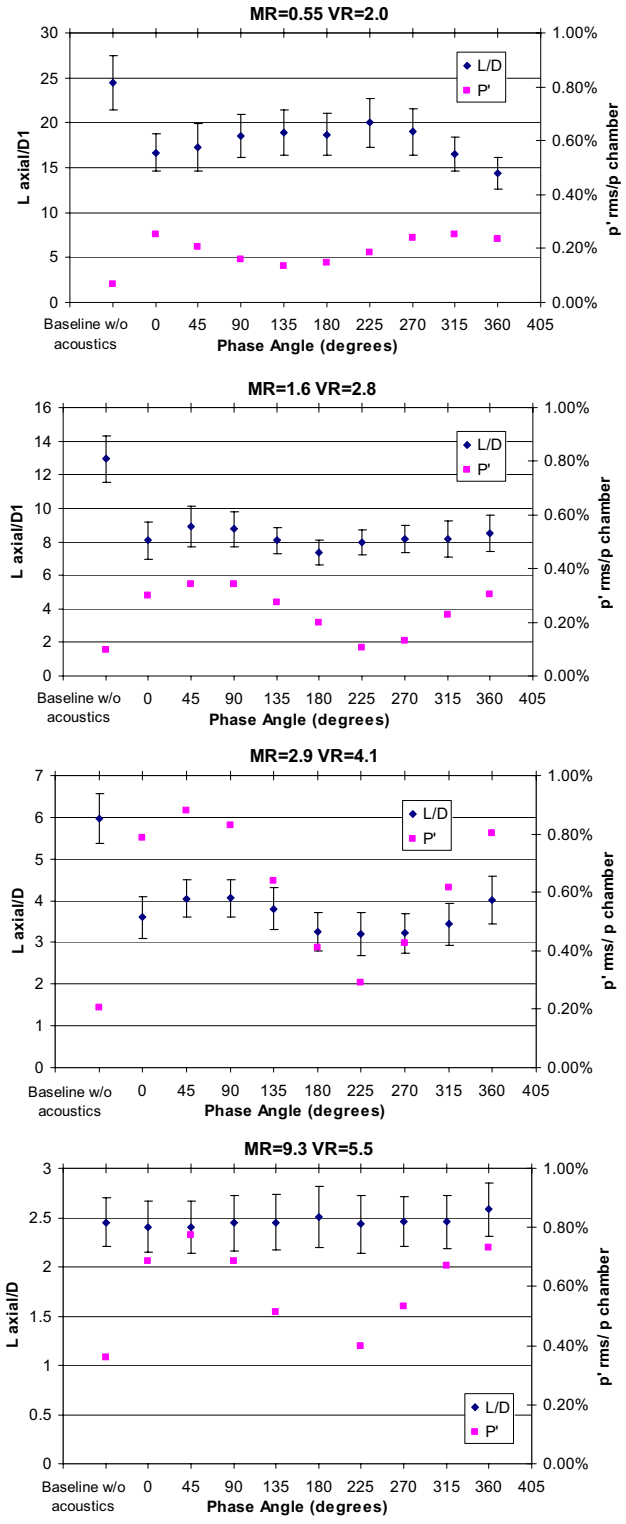

Figure 8. Comparison of acoustic pressure field and dark core length for nearcritical pressures and different MR's

other, as they should be since this represents a full cycle returning to the same point. Also note the p' baseline and the minimum value at 225 degrees are very close. In general, one would expect that when the two signals cancel each other, p' has the same value as the baseline with no acoustics, which represents the 'background' noise. In this case the range of maximum L/D is clustered around the maximum p' and the range of minimum L/D is clustered around the minimum p'. Although not shown, for the case with MR=4.9, VR=5.9, the same observations can be made. The last chart is for MR=9.3, VR=5.5. For this high MR, the dark core lengths are the smallest of all cases. The curve of L/D appears more flat. There does not seem to be a relation between the p' field and L/D. In fact, there is not a significant difference for L/D with and without acoustics. Therefore, the best qualitative agreement between L/D and p' was achieved for MR's between around 1-5.

We have seen in the previous observations for nearcritical pressures that acoustics affect the jet differently depending on the MR. For very low MR's the coaxial jet approaches the case of a single jet. In these cases, the inner jet barely acquires curvature due to the acoustic field. When MR is high enough (the specific threshold value depending on the chamber pressure) the recirculation zone set up in the region between the inner and the outer jet, due to the thick lip of the inner jet, becomes more prominent in the images and it starts to be of the same order of magnitude as the dark core itself. For these cases, when the jet is so short, the acoustics at any phase, move the jet back and forth but do not bend it. It also appears that for a given chamber pressure there is a range of MR's where the percentage change of the dark core length is maximum. For the case of subcritical pressures, it is ~1<MR~<4.

SUMMARY

In this paper we showed a complete set of data for a given geometry of a shear coaxial injector being perturbed by a transverse acoustic field. The acoustic field was set up by two acoustic sources. The phase angle of one acoustic source with respect to the other was changed from 0 degrees to 360 degrees. Three sets of operating chamber pressures spanning sub to supercritical values were chosen. For each chamber pressure an MR scan was done from MR <1 to MR >9. For all the pressure regimes, the cases with MR >9 were least sensitive to the acoustic field. That is, the percentage variation of the dark core length for those cases was least. At nearcritical pressures, for the cases with MR ~ 1 to 5 the trends of L/D qualitatively followed the p' field trends. That is, the maximum L/D was found around the maximum value of p' and vice versa. For these data, it seems like the dark core length is more affected, in terms of its reduction, by high acoustic velocity amplitude and not high acoustic pressure amplitudes.

ACKNOWLEDGMENT

The authors would like to thank Mr. Randy Harvey for his invaluable contributions in running and maintaining the facility and to Lt. Jeff Graham for his help with the data acquisition system and visualization technique. This work is sponsored by AFOSR under Mitat Birkan, program manager.

NOMENCLATURE

Symbol	Quantity	SI Unit
D	Diameter	mm
L	Dark core length	m
P	Pressure	Pa
T	Temperature	K
$\dot{m}$	Mass flux	mg/s
p'	Acoustic pressure	Pa
ρ	Density	kg/m^3
MR	Momentum flux ratio between outer and inner jet	dimensionless
VR	Velocity ratio between outer and inner jet	dimensionless

REFERENCES

1. Richecoeur, F., Scouflaire, P., Ducruix, S., Candel, S., High-Frequency Transverse Acoustic Coupling in a Multiple-Injector Cryogenic Combustor, *Journal of Propulsion and Power* 4:790-799 (2006).
2. Oschwald, M., Smith, J. J., Branam, R., Hussong, J., Schik, A., Chehroudi, B., Talley, D., Injection of Fluids into Supercritical Environments, *Combustion Science and Technology*, Vol. 178, No. 1-3, 2006, pp. 49-100.
3. Hulka, J., Hutt, J. J., *Liquid Rocket Engine Combustion Instability*, AIAA Progress in Astronautics and Aeronautics, Yang, V., Anderson W. E., Eds., 1995, p. 39-71.
4. Leyva, I. A., Rodriguez, J. I., Chehroudi, B., Talley, D., Preliminary Results on Coaxial Jets Spread Angles and the Effects of Variable Phase Transverse Acoustic Fields, AIAA-2008-0950
5. Rodriguez, J. I., Leyva, I. A., Chehroudi, B., Talley, D., Effects of a Variable-Phase Transverse Acoustic Field on a Coaxial Injector at Subcritical and Near-Critical Conditions, ILASS Americas, 21st Annual Conference on Liquid Atomization and Spray Systems, Orlando, Florida, May 18-21 2008
6. REFPROP, Reference Fluid Thermodynamic and Transport Properties, Software Package, Ver. 7.0, NIST, U.S. Department of Commerce, Gaithersburg, MD, 2002.
7. Thermophysical Properties of Fluid Systems (http://webbook.nist.gov/chemistry/fluid), NIST, U.S. Department of Commerce, Gaithersburg, MD, 2005
8. Otsu, N., *IEEE transactions on Systems, Man, and Cybernetics* 1:62-66 (1979).
9. Leyva, I. A., Chehroudi, B., Talley, D., Dark-core analysis of Coaxial Injectors at Sub-, Near-, and Supercritical Conditions in a Transverse Acoustic Field, *AIAA-2007-5456*
10. Leyva, I. A., Chehroudi, B., Talley, D., Dark-core analysis of Coaxial Injectors at Sub-, Near-, and Supercritical Conditions in a Transverse Acoustic Field, *54th JANNAF Meeting*, Denver, CO, May 14-18, 2007.

APPENDIX

Table 1. Run Conditions

	$T_{chamber}$ (K)	$\rho_{chamber}$ (kg/m^3)	$P_{chamber}$ (MPa)	T_{outer} (K)	$\dot{m}_{outer}$ (mg/s)	ρ_{outer} (kg/m^3)	u_{outer} (m/s)	T_{inner} (K)	$\dot{m}_{inner}$ (mg/s)	ρ_{inner} (kg/m^3)	u_{inner} (m/s)	Freq. (kHz)	$P'_{RMS\ max}$ (kPa)	VR	MR
SUB															
sub1	233	22.0	1.50	191	310	22.0	4.3	109	279	630	2.2	2.98	21.5	2.0	0.17
sub2	231	22.2	1.50	183	790	28.8	11	109	283	630	2.2	3.06	20.1	4.8	1.0
sub3	226	21.9	1.45	183	1230	27.8	16.9	109	284	630	2.2	3.06	17.8	7.6	2.6
sub4	226	22.9	1.51	185	1560	28.7	20.9	109	279	630	2.2	2.96	15.7	9.5	4.2
sub5	210	24.9	1.50	182	2400	29.3	31.3	109	279	630	2.2	3.01	16.9	14	9.6
sub6	216	24.1	1.50	191	3640	27.7	50.3	109	279	630	2.2	3.02	16.3	23	23
NEAR															
near1	223	56.6	3.58	180	1060	75.4	5.38	123	290	520	2.8	3.08	9.04	2.0	0.55
near2	207	62.0	3.57	152	1570	101	5.95	117	289	590	2.4	3.04	10.8	2.5	1.0
near3	228	55.1	3.58	185	1590	72.4	8.40	126	293	440	3.3	3.00	11.8	2.6	1.1
near4	223	56.1	3.55	184	2170	72.3	11.5	127	294	360	4.0	3.01	11.4	2.8	1.6
near5	230	54.2	3.56	199	2120	65.1	12.5	126	292	440	3.3	3.03	12.1	3.8	2.1
near6	229	54.5	3.56	183	2690	73.1	14.1	126	292	420	3.4	3.05	11.1	4.1	2.9
near7	219	57.6	3.56	194	3080	67.4	17.5	125	289	480	3.0	3.06	11.8	5.9	4.9
near8	213	59.6	3.56	192	6460	68.3	36.2	128	295	220	6.6	2.93	9.73	5.5	9.3
SUPER															
super1	231	76.1	4.96	198	292	93.9	1.19	136	291	300	4.8	3.05	8.01	0.25	0.019
super2	231	76.1	4.96	193	997	97.7	3.90	130	292	460	3.1	3.01	10.2	1.2	0.33
super3	221	80.4	4.95	180	2050	109	7.19	128	291	490	2.9	3.01	10.7	2.5	1.3
super4	222	80.1	4.96	182	3110	107	11.1	134	288	360	3.9	3.05	10.1	2.8	2.4
super5	222	80.3	4.97	191	2820	99.5	10.8	131	293	440	3.3	3.09	12.5	3.3	2.5
super6	211	85.8	4.96	187	5820	103	21.6	132	286	410	3.4	3.05	10.7	6.3	9.9